Chemistry–A European Journal
Research Article
doi.org/10.1002/chem.202402166
Chemistry Europe
European Chemical Societies Publishing
www.chemeurj.org

Investigations of Crucial Factors for the Non-Covalent Functionalization of Black Phosphorus (BP) using Perylene Diimide Derivatives for the Passivation of BP Nanosheets

Jasmin Eisenkolb,[a] Vicent Lloret,[a] Nathalie Zink-Lorre,[b] Sara Pla,[b] Gonzalo Abellán,[c] Ángela Sastre-Santos,[b] Frank Hauke,[a] Fernando Fernández-Lázaro,*[b] and Andreas Hirsch*[a]

The non-covalent functionalization of black phosphorus (BP) was studied with a scope of ten tailor-made perylene diimides (PDIs). A combination of UV/Vis-, fluorescence-, as well as Raman spectroscopy and atomic force microscopy was used to investigate the structural factors, which contribute to a pronounced PDI-BP interaction and thus support the protection of BP nanosheets against oxidative degradation. We were able to show, that water-soluble, amphiphilic PDIs with highly charged head groups can be used for the non-covalent functionalization of BP in aqueous media. Here, based on the hydrophobic effect, an efficient adsorption of the respective PDI molecules takes place and leads to the formation of a passivating film, yielding a considerable stabilization of the BP flakes under ambient conditions exceeding 30 days.

■■Dear author, please check if you can complete corresponding e-mails■■

Introduction

Black phosphorus (BP), the thermodynamically most stable allotrope of phosphorus[1] is, similar to graphene and traditional transition metal dichalcogenides, a layered material that can be delaminated.[2] Due to its unique properties, it is considered a potent representative of the novel class of 2D nanomaterials and has attracted an increasing interest over the past few years.[3] BP has an intrinsic band gap, a good combination of charge carrier mobility and current on/off ratio, as well as exhibits a unique in–plane anisotropy, making it an interesting candidate for applications in (opto−)electronics.[4–7]

Nevertheless, due to its electronic structure, BP is particularly susceptible to oxidation under ambient conditions, leading to the rapid degradation of the material. Especially mono- and few-layer nanosheets of BP are highly susceptible to the presence of oxygen, moisture and light irradiation.[8,9] To overcome these difficulties, various methods have been tested[10] like the covalent functionalization with aryl diazonium salts[10] or coordination using titanium sulfonate ligands,[12] which slow the degradation of BP by occupying the unpaired electrons at the surface. Other methods include the encapsulation of the material by depositing a protective layer on top of the BP nanosheets while maintaining the intrinsic properties of the material.[13,14] However, although encapsulation is an efficient passivation technique, further chemical modifications of the material are thus prevented.

Using a non-covalent approach for the passivation of the nanosheets offers a promising alternative for protecting BP, while simultaneously maintaining its intrinsic electronic properties. For other 2D materials, namely graphene[15] and MoS_2,[16] it could be shown that aromatic perylene diimides (PDIs) are suitable molecules for the formation of non-covalently functionalized hybrids. Perylene diimides are commonly known as a versatile class of chromophores, which are widely used as fluorescent dyes or color pigments[17–19] or in a diversity of optoelectronic applications such as dye lasers,[20,21] solar cells[22–24] or transistors[25,26] due to their excellent optical properties, especially with respect to their high fluorescence quantum yields and their photo- and thermal stability.[27–29] Moreover, these molecules possess a large conjugated π-system, rendering them ideal for the formation of supramolecular structures. This allows for the development of a passivating layer on top of the material and shows promising results for improving the device performance.[30–33] This rationale can likewise be transferred to BP.

Our group previously reported on the formation of BP-hybrids through non–covalent, van der Waals interactions between the BP nanosheets and different PDIs dissolved in organic media, and these hybrids showed an increased stability

[a] J. Eisenkolb, Dr. V. Lloret, Dr. F. Hauke, Prof. A. Hirsch
Chair of Organic Chemistry II, Center of Advanced Materials and Processes (ZMP), Friedrich-Alexander University Erlangen-Nürnberg, Dr.-Mack-Str. 81, 90762 Fürth
E-mail: andreas.hirsch@fau.de

[b] N. Zink-Lorre, Dr. S. Pla, Prof. Á. Sastre-Santos, Prof. F. Fernández-Lázaro
Área de Química Orgánica, Instituto de Bioingeniería, Universidad Miguel Hernández, Avda. de la Universidad s/n, 03203 Elche, Spain
E-mail: ■■email missing■■

[c] G. Abellán
Instituto de Ciencia Molecular (ICMol), Universidad de Valencia, Catedrático José Beltrán 2, 46980 Paterna, Spain

Supporting information for this article is available on the WWW under https://doi.org/10.1002/chem.202402166

under ambient conditions due to the passivating effect of the PDI layer.[34,35] Moreover, PDIs provide the opportunity to modify their structure by attaching a variety of functional groups at three different positions of the perylene core (indicated in Scheme 1), influencing their optical properties, their solubility, as well as their supramolecular behavior including aggregation.[36–38]

Substituents in the imide position are able to directly influence the solubility along with the self-assembly of the molecules, however, they have nearly no effect on the HOMO (highest occupied molecular orbital) and LUMO (lowest unoccupied molecular orbital) of the molecule, rendering changes in the absorption and emission properties neglectable.[39] Bay substitution, on the other hand, primarily influences the optical properties of the corresponding PDI. Introduction of π-acceptor or π-donor substituents leads to either a lowering of the LUMO or a raising of the HOMO, resulting in both cases in a bathochromic shift of the absorption features.[40] However, bay substitution often leads to the twisting of the otherwise planar core. Introducing substituents in the ortho positions of the perylene can enhance its solid–state emission and affect the solubility without distorting the planar structure.[41,42] Hence, the introduction of different functional moieties in various positions of the PDI core offers a wide variety of modification potential.

These alterations seem to influence the non-covalent interactions between the corresponding PDI and BP, which could be shown in the thermal stability of the functionalized nanosheets depending on the strength of the non-covalent interaction.[35] However, detailed insights by which means the successful formation of such hybrid structures can be influenced, remain elusive.

Herein, we present a thorough, systematic investigation of ten structurally–different PDIs towards their potential for the non–covalent functionalization and passivation of BP. Modifications in either the imide, the bay or the ortho positions of the perylene core were explored, which influence their physicochemical properties, rendering the PDIs either water–soluble, exhibiting electron donating or electron withdrawing character, twisting the planar core structure or elongating the π-system. This enables a deeper, fundamental understanding of the interactions between PDIs and BP and how they can be modified on demand.

Results and Discussion

As outlined, the exact chemical structure of substituted perylene diimides has a significant impact on various properties, like their polarity, solubility and aggregation behavior. Therefore, the intrinsic solution-phase behavior of the respective PDIs was investigated at first and the subsequently obtained BP-PDI hybrids were thoroughly characterized and investigated towards their ability to stabilize pristine BP over time under ambient conditions. A straightforward and facile method to examine the aggregation behavior of different PDIs in solution is the combination of absorption and fluorescence spectroscopy.

Based on the previously obtained results for the passivation of BP nanosheets with organic PDIs (**PDI-Ref**, Scheme 2),[34,35] certain molecular structures were designed to probe the influence of specific molecular characteristics. To identify possible influences on the non–covalent interaction with BP, three structurally different PDIs (Scheme 2) were selected and tested, which were either elongated with branched alkyl chains (**PDI 1**), feature polar groups in the ortho positions of the core (**PDI 2**) or exhibit an extended π–system by further elongating the PDI in ortho positions with phenylacetylene units (**PDI 3**). All PDI derivatives can be readily dissolved in THF.

As mentioned above, modifications in the imide positions of a PDI have nearly no influence on its photophysical properties, however, they do affect the intermolecular stacking behavior and thereby influence phenomena such as aggregation–induced fluorescence quenching.[43] Therefore, a simple, branched alkyl chain was selected for all three PDIs, which differs from the presented **PDI-Ref** mostly in its polarity, and the aggregation behavior of these PDIs was investigated. **PDI-Ref**, which is literature–known to successfully form non-covalent hybrids with BP, showed signs of aggregation in THF, which can be clearly discerned by the low A_{0-0}/A_{0-1} ratio and the additional band at 552 nm, indicating H–aggregates due to van der Waals interactions (see Supporting Information of Ref. [35]). The corresponding fluorescence spectrum, however, revealed three, distinct peaks, which is usually characteristic for monomeric solutions.[35] In comparison, **PDI 1** exhibits a characteristic absorption spectrum, whereas three distinct absorption maxima are visible that increase in intensity with

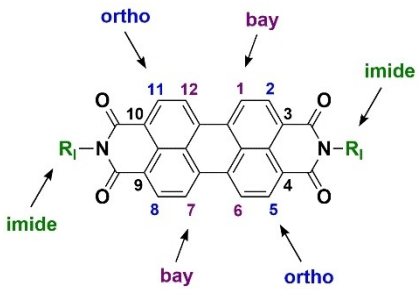

Scheme 1. General structure of a PDI with highlighted substitution positions.

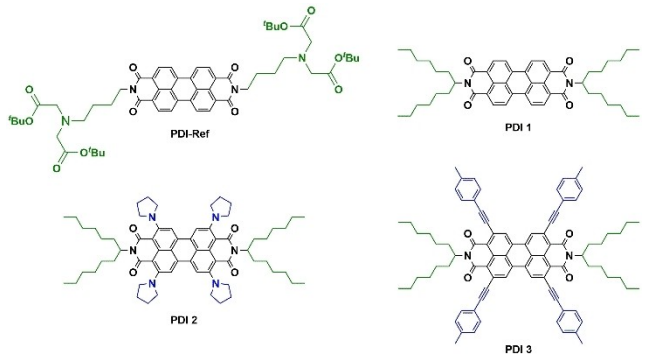

Scheme 2. Chemical structures of the investigated PDIs (**PDI 1** to **PDI 3**) soluble in organic solvents and the previously investigated **PDI-Ref**. [34,35].

lower energy. The corresponding fluorescence spectrum is a clear mirror image, confirming its monomeric behavior in solution. However, **PDI 2** shows the complete opposite (Supporting Information, S1). Both, UV/Vis and fluorescence spectra, reveal significant aggregation due to the broadening of the absorption peaks and the additional shoulder at around 542 nm. Finally, **PDI 3** emerges as the derivative most similar to **PDI-Ref** in terms of its optical characterization. Although the absorption spectrum suggests some degree of aggregation, an additional shoulder at higher wavenumbers is absent and the fluorescence spectrum reveals three distinct peaks, as already observed for **PDI-Ref**, rendering it the most promising candidate for the non–covalent functionalization of BP due to their spectral similarities (Supporting Information, S1).

The non-covalent functionalization between these PDIs and BP was then investigated in detail. Therefore, few–layer BP (FL–BP) was obtained *via* micromechanical exfoliation of bulk BP crystals under inert conditions inside an argon-filled glovebox ($O_2 < 0.1$ ppm, $H_2O < 0.1$ ppm) and transferred onto Si/SiO_2 wafers for further processing. These wafers were immersed in the corresponding PDI solution ($c = 10^{-5}$ mol/L in THF) for 5 days. To investigate the potential PDI-BP hybrid formation, the wafers were washed with isopropanol and Raman spectroscopy was used to verify the success of the non-covalent functionalization (Scheme 3).

As briefly outlined above, **PDI 1** showed a typical absorption and fluorescence behavior for perylenes, indicated by the three visible absorption peaks and its mirror image in the fluorescence spectrum (Figure 1a). This optical characteristic suggests a monomeric stacking behavior, which can be confirmed by calculating the corresponding ratio between the first and the second highest absorption peak. If this ratio is around or above a value of 1.6, nearly to no aggregation of the molecules is present, (Supporting Information, T1).[44] However, although no pre–arrangement of the molecules takes place which could prevent a potential interaction with the BP nanosheets, no indications for a successful non–covalent functionalization could be found by Raman spectroscopy, which becomes evident by the missing signals in the spectral range from 1200 cm^{-1} to 1800 cm^{-1} (Figure 1b). This could indicate that a purely monomeric behavior of the PDI molecules is not favorable for their interaction with BP, which is in accordance with findings reporting lower exfoliation tendencies of graphite with purely monomeric PDIs as the exfoliation agent.[45,46] High degrees of self–assembly of the PDI molecules in solution suggest reduced interaction potential with BP, however, instead it appears that the functional group at the imide position and its polarity could have a greater influence on the improvement of the van der Waals interaction between the π–system of the perylene and the BP surface.

To investigate, whether the polar groups are specifically needed in the imide position of the PDI core or if they are favorable for the non–covalent interaction in general, **PDI 2** was tested, which bears polar pyrrolidine units in ortho position. In comparison to **PDI 1**, the solution showed a high degree of aggregation, which can be clearly seen by the overlapping of the three absorption maxima of the PDI core, yet no signs for the non-covalent functionalization of BP could be detected (Supporting Information, S1). This suggests, that it might be necessary for the PDI to either harbor polar headgroups in at least the imide position or for an additional driving force to be present to increase the chances for the non–covalent interaction.

Therefore, **PDI 3** was investigated, which exhibits an extended, planar π–system by introducing phenyl acetylene units in the ortho positions of the PDI core. These substituents are located in the same plane as the perylene core, further delocalizing the electrons into the substituents, hence improving and strengthening the van der Waals interactions between the BP nanosheets and each individual PDI molecule. Its optical characterization reveals a noticeable aggregation in solution (Figure 2a). Interestingly however, the fluorescence spectrum resembles that of **PDI 1**, which was obtained from a monomeric solution, similar to the published results of **PDI-Ref**. [35].

Using **PDI 3** for the non–covalent functionalization of BP led to the successful formation of PDI–BP hybrids, which can be clearly observed by Raman spectroscopy showing the characteristic PDI bands between 1200 cm^{-1} and 1800 cm^{-1} due to the fluorescence quenching resulting from the non-covalent inter-

Scheme 3. Schematic representation of the non-covalent functionalization procedure of BP with PDIs.

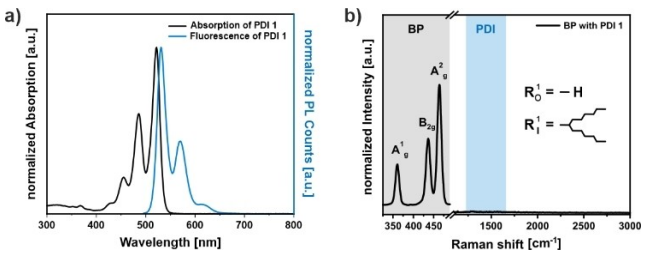

Figure 1. Optical properties of **PDI 1** characterized by (a) UV/Vis and fluorescence spectroscopy and (b) the corresponding Raman spectrum of an exemplary BP flake after the non-covalent functionalization with **PDI 1** (organic rests are marked with the letter O for ortho- and with I for imide substituents).

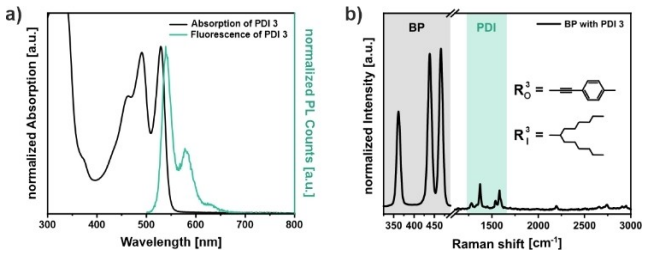

Figure 2. Optical properties of **PDI 3** characterized by (a) UV/Vis and fluorescence spectroscopy and (b) the corresponding Raman spectrum of an exemplary BP flake after the non-covalent functionalization with **PDI 3** (organic rests are marked with the letter O for ortho- and with I for imide substituents).

action (Figure 2b). This is in good accordance with our previous results.[34,35]

The newly formed BP-**PDI 3** hybrid was characterized in more detail by atomic force microscopy (AFM) as depicted in Figure 3. The respective AFM images of a selected flake with a thickness of around 7 nm recorded over a time span of 18 days shine light on the passivating capabilities of **PDI 3** under ambient conditions, which could confirm a prolonged lifetime of the BP-**PDI 3** hybrids. Usually, in the first few hours after exposing BP to air, the formation of small droplets on the surface of the monitored flake can be observed. These droplets arise from the formation of hydrophilic P_xO_y species due to the chemisorption of oxygen, which, little by little, increases the hydrophilicity of the BP surface.[47] This leads to the adsorption of water and the subsequent formation of phosphoric and phosphorus acids, which can be confirmed by the appearance of visible droplets.[48] For the BP–**PDI 3** hybrid, this process starts most noticeably after seven days under ambient conditions (Figure 3d), which clearly indicates an efficient shielding effect of the non-covalently adsorbed **PDI 3** against oxygen and moisture. However, it has to be stated, that using a similar PDI to **PDI-Ref** (published by Lloret *et al.*[35]), which interacts more strongly with BP, the time span can be extended to a far larger extent. To completely passivate BP from oxygen and water, at least six monolayers of PDI are necessary according to molecular dynamic simulations, which equals about 1.3 nm in thickness.[35,49] Such PDI layer thicknesses have already been reported using three different PDIs, where the observed BP flakes showed a higher thickness after non-covalent functionalization of about 1–2 nm depending on the used method.[34,35] As seen in the AFM height comparison (Figure 3c and d), the BP flake, taken from Figure 3 of the manuscript, reveals a height increase after the non-covalent functionalization of about 0.6 nm, which should according to Lloret *et al.*[35] account to about three monolayers of PDI. This would explain the shorter lifetime of about 7 days of the observed BP flake, as this is less PDI than the minimum requirement for a complete passivation.

All of the abovementioned PDIs showed substitutions in the imide or the ortho positions of the perylene core. The influence of bay substitution on the non-covalent interaction of PDIs with BP, however, has not been investigated yet. It is well-known, that the substitution in ortho or bay position has a significant impact on the electronic structure and the optical properties of the corresponding PDIs, leading to bathochromic or hypsochromic shifts in the absorption and emission spectra of even up to 150 nm compared to unsubstituted PDIs and in most cases, influences of bay substitution prevail.[40,50] For this reason, the difference between ortho and bay substitution was further investigated on the basis of **PDI 4** and **PDI 5** (Scheme 4). Since bay substitution is especially tricky due to steric hindrance, only small groups could be tested.

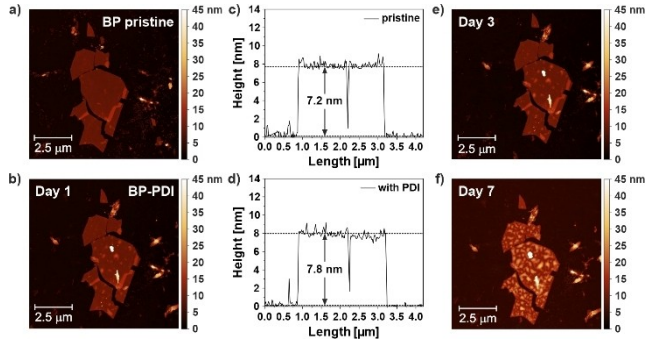

Figure 3. AFM images of pristine BP flakes (a) before and (b) after the non–covalent functionalization with **PDI 3** and the corresponding height profiles of the flake (c–d). (e–f) AFM stability study of the BP flakes shown in (b) over time.

The measured UV/Vis and fluorescence spectra of the bay substituted **PDI 5** show overlapping absorption and emission maxima, although the A_{0-0}/A_{0-1} ratios between **PDI 4** and **PDI 5** do not differ significantly (Supporting Information, T1). This indicates only a slight aggregation in solution. However, both PDIs show no signs for a successful non–covalent functionalization of BP (Supporting Information, S2). As already demonstrated for **PDI 2**, solely ortho substitution of the perylene core does not automatically lead to a pronounced van der Waals mediated stacking between the corresponding PDI core and BP if no additional driving force is introduced. Furthermore, it is widely known that bay substitution distorts the otherwise planar perylene core,[51–53] which could lead to reduced van der Waals interactions with the BP nanosheets, explaining the observed results. The experimental data for two additional PDIs (**PDI 6** and **PDI 7**), which showed only minor structural changes compared to the presented ones, can be found in the Supporting Information (Figure S3).

In contrast to the already mentioned PDIs, which can be readily dissolved in a variety of organic solvents, changing the substituents at the imide positions moreover allows for the synthesis of water-soluble PDIs, which have been widely investigated[54–58] and few reports show their use for the formation of non-covalent aggregates with 2D materials like reduced graphene oxide (rGO),[59] carbon nanotubes and graphene.[60–62] Using water-soluble PDIs for the passivation of BP, which is known to be a moisture-sensitive material, seems counterintuitive at first, however, they might offer additional driving forces for the non-covalent interaction due to their amphiphilic nature. Our group previously showed, that BP can be sequentially thinned by removing hydrophilic P_xO_y species by water rinsing, recovering a pristine BP surface.[63] Subsequent non-covalent functionalization of the thinned BP with **PDI-Ref** led to the successful passivation of the surface. In addition, it was observed that rinsing the BP surface with water in short intervals leads to an overall slower oxidation compared to leaving the nanosheets for four days under ambient conditions. This is in accordance with previous findings, which suggested

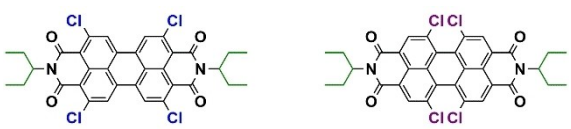

PDI 4 PDI 5

Scheme 4. Chemical structures of **PDI 4** and **PDI 5** dissolved in THF.

that the hydrophobic surface of BP needs to be oxidized first to generate a hydrophilic environment for the subsequent physisorption of water.[64,65] Therefore, FL-BP can survive for a significantly longer time in deoxygenated water.[66]

In our present study, PDIs are modified in the imide position by introducing permanently charged functionalities like quaternary ammonium cations (**PDI 8**) or N–oxides (**PDI 9**) or by using pH–dependent dendritic carboxylic acid motifs (**PDI 10**).

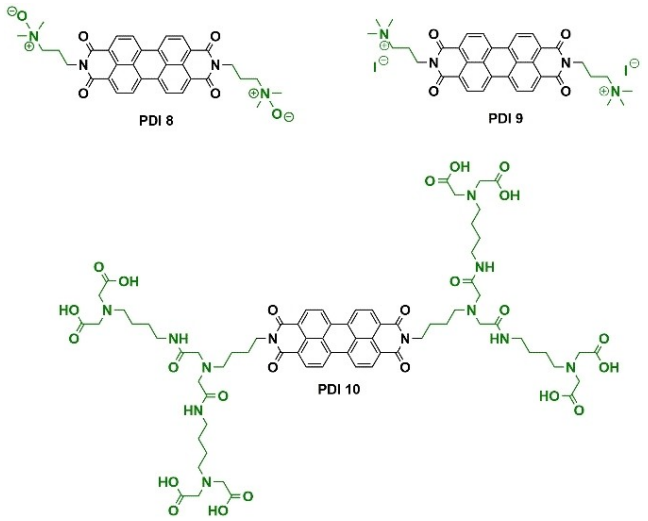

Scheme 5. Chemical structures of the investigated water-soluble PDIs.

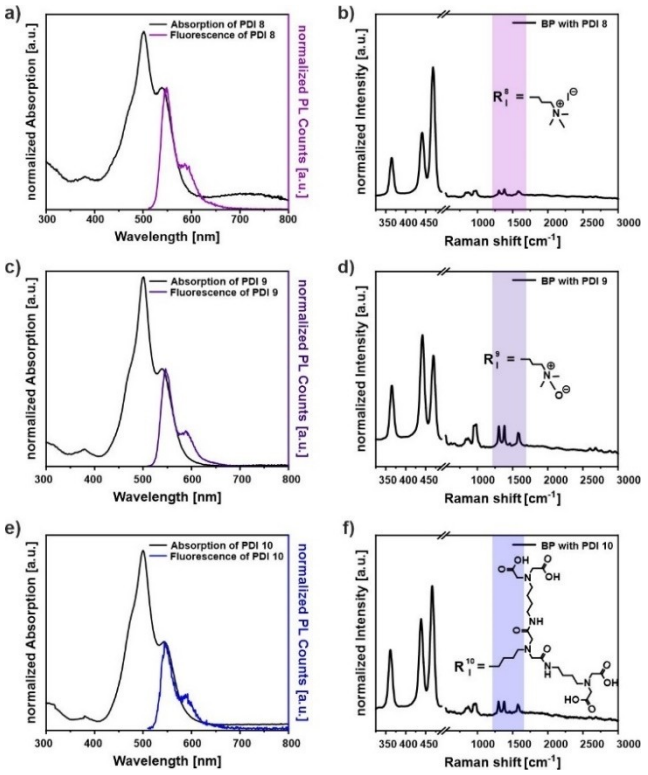

Figure 4. Optical properties of (a) **PDI 8**, (c) **PDI 9** and (e) **PDI 10** characterized by UV/Vis and fluorescence spectroscopy and (b), (d) and (f) the corresponding Raman spectrum of an exemplary BP flake after the non-covalent functionalization with the indicated PDIs.

■■Dear author, please mention (Scheme 5■■

These modifications allow the aforementioned PDIs to be dissolved in water and although such PDIs have been known for quite some time, they have never been used for the non-covalent functionalization of BP. Therefore, we investigated **PDI 8–10** with regard to their ability to form non–covalent hybrid structures with BP, as well as their potential in passivating the nanosheets.

The same approach as described above was used, however, water as the solvent was deoxygenated to minimize BP oxidation during the immersion, which led to the successful formation of the non-covalently functionalized BP nanosheets for all three compounds. This was confirmed by Raman spectroscopy, showing characteristic bands of the PDI structure between 1200 cm^{-1} and 1800 cm^{-1} (Figure 4).

Clear differences can be determined by comparing the PDIs dissolved in organic solvents with the aforementioned water–soluble ones. The molecular structure of the used PDIs has a tremendous influence on the capability of the PDI to develop van der Waals mediated interactions with BP, however, their aggregation behavior seems to play only a subordinate role, confirming that the non-covalent functionalization of BP is indeed influenced by multiple factors, making predictions about its success solely based on aggregation impractical. The introduction of a planar, π–extended system seems to be necessary for a successful non-covalent functionalization in organic solvents, whereas the chain length in the imide position or electron withdrawing or donating substituents in ortho position appear to have a neglectable influence. In comparison to the **PDIs 1**–**7**, which showed a clear preference for molecules with extended π-systems, the interaction between the perylene core and BP in the water-soluble, amphiphilic PDI derivatives is mainly driven by the hydrophobic effect. The hydrophilic, polar head group is responsible for the excellent water solubility of the entire molecule and the hydrophobic core tends to aggregate in order to minimize the total energy of the system. This assumption is supported by the recorded UV/Vis and fluorescence spectra, from which a high aggregation tendency can be derived. In Figure 4 (left side), this aggregation becomes visible based on the overlap and broadening of the three distinct absorption bands of the perylene units and the low A_{0-0}/A_{0-1} ratios.[44] However, similar to **PDI 3** in THF, the photoluminescence response is quite pronounced and the subsequent Raman measurement confirms the successful non-covalent functionalization of BP with every tested water–soluble PDI.

Since **PDI 10** showed strong Raman signals, it was used as a model compound to investigate the passivation capability of water–soluble PDIs in detail. As mentioned above, atomic force microscopy can be used to shine light on the oxidation behavior of these BP-**PDI 10** hybrids (Figure 5).

The recorded Raman maps, depicting the A^1_g band of BP and the PDI band at 1302 cm^{-1}, and the AFM image taken directly after the non-covalent functionalization of the shown BP flakes with the water-soluble **PDI 10** (Figure 5a–c), reveal uniform PDI signals over the whole BP flakes, confirming the successful interaction between the PDI molecules and BP, while

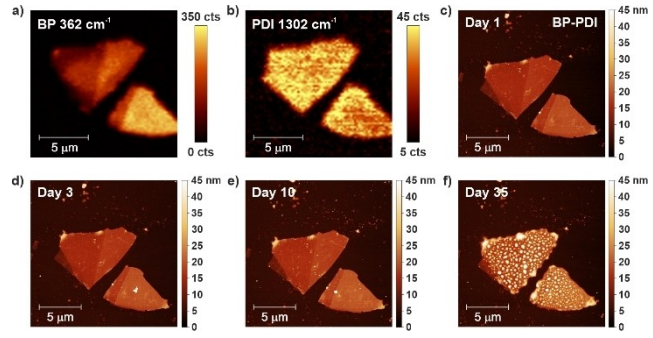

Figure 5. Characterization of non-covalently functionalized BP flakes with **PDI 10** by Raman spectroscopy and AFM. Raman maps illustrate (a) the A^1_g band of BP and (b) one PDI band at 1302 cm^{-1} and (c) shows the corresponding AFM image. (d–f) AFM stability study of the BP flakes shown in (c) with **PDI 10** over time.

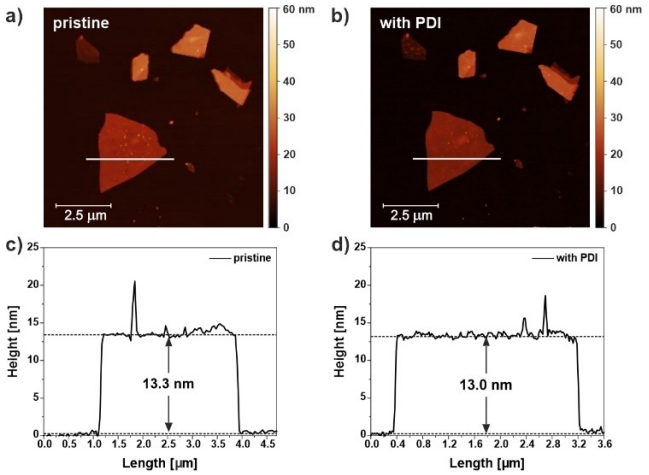

Figure 6. AFM images of a pristine BP flake (a) before and (b) after the non–covalent functionalization with **PDI 10**. (c) and (d) show the corresponding height profile of the indicated flake.

the Raman signals of BP and the surface topology remain unaffected. The stability of the observed flakes was tracked by AFM. After the first ten days under ambient conditions, no significant change in the surface topography can be determined and even after 35 days, only a light nanobubble formation can be observed. In comparison to pristine BP, which deteriorates already after the first few hours upon exposure to air,[48,67] and to the non-covalently functionalized nanosheets presented in Figure 3, the stability of the BP nanosheets can be tremendously increased to over a month under ambient conditions, demonstrating the simplicity and efficiency of the presented method.

The determination of the exact height of the observed flakes after functionalization is quite challenging, as the flakes have nearly the same thickness as measured before the functionalization. Our group previously explained this behavior by a layer-by-layer oxidation of the material in water.[63] This allows for control over the thickness of the BP nanosheets and leads to a gradual thinning of the material with each washing step. This process can be terminated by either using the ionic liquid BMIM–BF_4 as a passivating layer or by non-covalently functionalizing the nanosheets with PDIs, forming a protective barrier against further oxidation.

This can be adapted to this experiment as well. The presence of water and small traces of oxygen in the solvent act as the oxidizing agent and the as-formed phosphoric and phosphorous acids are subsequently washed away from the surface, leading to a slight thinning of the flakes immediately before they are functionalized in the same solution. This results in nearly to no changes in the overall height of a flake after the functionalization (Figure 6).

Conclusions

In conclusion, we have presented a thorough investigation of overall ten structurally different PDIs with regard to their aggregation behavior in solution and their non-covalent interaction with black phosphorus nanosheets, which is summarized in the Supporting Information for a better overview over the obtained results (Tables T1 and T2. We could show, that besides imide position substituted perylene diimide derivatives, also ortho-substituted systems with extended π–systems are promising candidates for the non-covalent functionalization of BP. In addition, they show auspicious results for a subsequent passivation and stabilization of the nanosheets against oxidative degradation. Moreover, we have demonstrated, that water–soluble, amphiphilic PDIs with highly charged head groups can be used for the non-covalent functionalization of BP in an aqueous medium. Here, based on the hydrophobic effect, an efficient adsorption of the respective PDI molecules takes place, which leads to the formation of a passivating film, stabilizing the BP nanosheets on a long-term basis. Our findings stress once more the extraordinary properties of perylene diimides for the formation of supramolecular hybrid structures and this approach might pave the way for future applications of BP.

Experimental

Sample Preparation

Black phosphorus (BP) crystals were mechanically exfoliated using a sticky polymer tape and transferred to Si/SiO_2 to yield few-layer BP. These pristine samples were immersed in various PDI solutions (PDI 1–10, $c = 10^{-5}$ mol/L) in three organic solvents, namely NMP, DCM, THF and in water. After 5 days of immersing, the wafer were put out of the solutions, were dried and cleaned by sonication in isopropanol for 1 min to remove possible PDI residues and aggregates.

Solvent Preparation

Commercially available anhydrous THF and the bidistilled water used for the fabrication of the PDI solutions was purified beforehand. Both solvents were pump-freezed at least five times to exclude the presence of oxygen.

Scanning Probe Microscopy

AFM images were recorded using a Bruker Dimension Icon 3 microscope in ScanAsyst Air mode. AFM topography images were obtained with Bruker ScanAsyst-Air silicon tips on nitride levers coated with reflective aluminum and a spring constant of 0.4 $N\,m^{-1}$, resolved by either 512×512 pixels or 1024×1024 pixels and with a scan rate of 0.4 Hz.

Raman Spectroscopy

Raman spectra and maps were acquired on a WITec alpha300 R confocal microscope equipped with an automated XYZ stage. All Raman measurements were conducted using an excitation wavelength of 532 nm and the non-covalent functionalization of BP with various PDIs was verified by Single Raman spectra, recorded for various flakes across the wafer with 5 mW laser power, an integration time of 0.2 s and 10 accumulations.

UV/Vis Spectroscopy

Absorption of the prepared PDI solutions was measured on a Perkin Elmer Lambda 1050 spectrometer in quartz cuvettes with a path length of 0.4 cm.

Fluorescence

Emission spectra were acquired on a Horiba Scientific Fluorolog–3 system equipped with 450 W xenon halogen lamp, double monochromator in excitation (grating 600 lines/mm blazed at 500 nm) and emission (grating 1200 lines/mm blazed at 500 nm), and a PMT (photomultiplier tube) detector using quartz cuvettes with a path length of 1.0 cm.

Supporting Information Summary

The Supporting Information section includes the experimental protocols, additional information on the respective PDIs and UV/Vis- and fluorescence spectra. The authors have cited additional references within the Supporting Information.[67–72]

Acknowledgements

The research leading to these results was partially funded by the European Research Council (ERC Advanced Grant 742145 B-PhosphoChem (A.H.) and ERC Starting Grant No. 2D-Pnicto-Chem 804110 (G.A.)). The authors (J.E., V.L., F.H., A.H.) would like to thank the Deutsche Forschungsgemeinschaft (DFG, German Research Foundation) for financial support in scope of the Collaborative Research Centre SFB 953 "Synthetic Carbon Allotropes" (Project-ID 182849149, project A1), the FLAG-ERA AB694/2-1 (G.A.), as well as the Graduate School Molecular Science (GSMS). This research (G.A., N.Z.-L., S.P., Á.S.-S., F.F.-L.) was also financed by Grant PID2022-143297NB-I00, MRR/PDC2022-133997I00, TED2021-131347B-I00, Unit of Excellence "Maria de Maeztu" CEX2019-000919-M, (to G.A.) and PID2022-140315NB-I00 funded by MICIU/AEI/10.13039/501100011033 and by ERDF/EU (to FF–L) and the Generalitat Valenciana (CIDEGENT/2018/001, CIPROM/2021/059) and the Advanced Materials program by MCIN with funding from European Union NextGenerationEU (PRTR-C17.I1) and Generalitat Valenciana (MFA/2022/028). Open Access funding enabled and organized by Projekt DEAL.

Conflict of Interests

The authors declare no conflict of interest.

Data Availability Statement

The data that support the findings of this study are available from the corresponding author upon reasonable request.

Keywords: Non-covalent functionalization · Passivation · Perylene diimides · Phosphorus · Supramolecular chemistry

[1] J. Sun, G. Zheng, H. W. Lee, N. Liu, H. Wang, H. Yao, W. Yang, Y. Cui, *Nano Lett.* **2014**, *14*, 4573–4580.
[2] F. Xia, H. Wang, J. C. M. Hwang, A. H. C. Neto, L. Yang, *Nat. Rev. Phys.* **2019**, *1*, 306–317.
[3] R. Gusmão, Z. Sofer, M. Pumera, *Angew. Chem. Int. Ed.* **2017**, *56*, 8052–8072.
[4] H. Liu, A. T. Neal, Z. Zhu, Z. Luo, X. Xu, D. Tománek, P. D. Ye, *ACS Nano* **2014**, *8*, 4033–4041.
[5] M. Engel, M. Steiner, P. Avouris, *Nano Lett.* **2014**, *14*, 6414–6417.
[6] M. Buscema, D. J. Groenendijk, S. I. Blanter, G. A. Steele, H. S. J. Van Der Zant, A. Castellanos-Gomez, *Nano Lett.* **2014**, *14*, 3347–3352.
[7] Y. Zhou, M. Zhang, Z. Guo, L. Miao, S. T. Han, Z. Wang, X. Zhang, H. Zhang, Z. Peng, *Mater. Horiz.* **2017**, *4*, 997–1019.
[8] Y. Huang, J. Qiao, K. He, S. Bliznakov, E. Sutter, X. Chen, D. Luo, F. Meng, D. Su, J. Decker, W. Ji, R. S. Ruoff, P. Sutter, *Chem. Mater.* **2016**, *28*, 8330–8339.
[9] A. Favron, E. Gaufrès, F. Fossard, A.-L. Phaneuf-L'Heureux, N. Y. W. Tang, P. L. Lévesque, A. Loiseau, R. Leonelli, S. Francoeur, R. Martel, *Nat. Mater.* **2015**, *14*, 826–832.
[10] Y. Chen, L. Xu, W. Li, W. Wan, Z. Song, S. Zhao, Z. Ling, P. Li, S.-Y. Zhang, N. Arif, Y.-J. Zeng, *J. Phys. Condens. Matter* **2022**, *34*, 224004.■■Please check and confirm the edit made, and correct if necessary.■■
[11] C. R. Ryder, J. D. Wood, S. A. Wells, Y. Yang, D. Jariwala, T. J. Marks, G. C. Schatz, M. C. Hersam, *Nat. Chem.* **2016**, *8*, 597–602.
[12] Y. Zhao, H. Wang, H. Huang, Q. Xiao, Y. Xu, Z. Guo, H. Xie, J. Shao, Z. Sun, W. Han, X.-F. Yu, P. Li, P. K. Chu, *Angew. Chem. Int. Ed.* **2016**, *55*, 5003–5007.
[13] Y. Y. Illarionov, M. Waltl, G. Rzepa, J.-S. Kim, S. Kim, A. Dodabalapur, D. Akinwande, T. Grasser, *ACS Nano* **2016**, *10*, 9543–9549.
[14] S. Gamage, A. Fali, N. Aghamiri, L. Yang, P. D. Ye, Y. Abate, *Nanotechnology* **2017**, *28*, 265201.
[15] N. C. Berner, S. Winters, C. Backes, C. Yim, K. C. Dümbgen, I. Kaminska, S. Mackowski, A. A. Cafolla, A. Hirsch, G. S. Duesberg, *Nanoscale* **2015**, *7*, 16337–16342.
[16] H. Kim, W. Kim, M. O'Brien, N. McEvoy, C. Yim, M. Marcia, F. Hauke, A. Hirsch, G.-T. Kim, G. S. Duesberg, *Nanoscale* **2018**, *10*, 17557–17566.
[17] Y. Avlasevich, C. Li, K. Müllen, *J. Mater. Chem.* **2010**, *20*, 3814–3826.
[18] E. Rostami-Tapeh-Esmail, M. Golshan, M. Salami-Kalajahi, H. Roghani-Mamaqani, *Dyes Pigm.* **2020**, *180*, 108488.
[19] F. Würthner, *Chem. Commun.* **2004**, 1564–1579.■■Please provide volume number■■
[20] M. Sadrai, G. R. Bird, *Opt. Commun.* **1984**, *51*, 62–64.
[21] M. G. Ramírez, S. Pla, P. G. Boj, J. M. Villalvilla, J. A. Quintana, M. A. Díaz-García, F. Fernández-Lázaro, Á. Sastre-Santos, *Adv. Opt. Mater.* **2013**, *1*, 933–938.
[22] H. Choi, S. Paek, J. Song, C. Kim, N. Cho, J. Ko, *Chem. Commun.* **2011**, *47*, 5509–5511.

[23] G. D. Sharma, M. S. Roy, J. A. Mikroyannidis, K. R. Justin Thomas, *Org. Electron.* **2012**, *13*, 3118–3129.
[24] H. Hu, Y. Li, J. Zhang, Z. Peng, L. Ma, J. Xin, J. Huang, T. Ma, K. Jiang, G. Zhang, W. Ma, H. Ade, H. Yan, *Adv. Energy Mater.* **2018**, *8*, 1800234.
[25] R. Schmidt, M. M. Ling, J. H. Oh, M. Winkler, M. Könemann, Z. Bao, F. Würthner, *Adv. Mater.* **2007**, *19*, 3692–3695.
[26] R. Schmidt, J. H. Oh, Y.-S. Sun, M. Deppisch, A.-M. Krause, K. Radacki, H. Braunschweig, M. Könemann, P. Erk, Z. Bao, F. Würthner, *J. Am. Chem. Soc.* **2009**, *131*, 6215–6228.
[27] H. Langhals, *Heterocycles* **1995**, *40*, 477–500.
[28] N. Soh, T. Ueda, *Talanta* **2011**, *85*, 1233–1237.
[29] A. Nowak-Król, F. Würthner, *Org. Chem. Front.* **2019**, *6*, 1272–1318.
[30] H. Yu, P. Joo, D. Lee, B.-S. Kim, J. Hak Oh, H. Yu, D. Lee, J. H. Oh, P. Joo, B. Kim, *Adv. Opt. Mater.* **2015**, *3*, 241–247.
[31] T. Huang, D. Lu, L. Ma, X. Xi, R. Liu, D. Wu, *Chem. Eng. J.* **2018**, *349*, 66–71.
[32] J. Yang, H. Miao, Y. Wei, W. Li, Y. Zhu, *Appl. Catal. B* **2019**, *240*, 225–233.
[33] Y. Sheng, H. Miao, J. Jing, W. Yao, Y. Zhu, *Appl. Catal. B* **2020**, *272*, 118897.
[34] G. Abellán, V. Lloret, U. Mundloch, M. Marcia, C. Neiss, A. Görling, M. Varela, F. Hauke, A. Hirsch, *Angew. Chem. Int. Ed.* **2016**, *55*, 14557–14562.
[35] V. Lloret, E. Nuin, M. Kohring, S. Wild, M. Löffler, C. Neiss, M. Krieger, F. Hauke, A. Görling, H. B. Weber, G. Abellán, A. Hirsch, *Adv. Mater. Interfaces* **2020**, *7*, 2001290.
[36] C.-W. Chang, H.-Y. Tsai, K.-Y. Chen, *Materials* **2014**, *7*, 5488–5506.
[37] F. Würthner, C. R. Saha-Möller, B. Fimmel, S. Ogi, P. Leowanawat, D. Schmidt, *Chem. Rev.* **2016**, *116*, 962–1052.
[38] R. K. Dubey, S. J. Eustace, J. S. van Mullem, E. J. R. Sudhölter, F. C. Grozema, W. F. Jager, *J. Org. Chem.* **2019**, *84*, 9532–9547.
[39] R. S. Wilson-Kovacs, X. Fang, M. J. L. Hagemann, H. E. Symons, C. F. J. Faul, *Chem. Eur. J.* **2022**, *28*, e202280361.
[40] C. Huang, S. Barlow, S. R. Marder, *J. Org. Chem.* **2011**, *76*, 2386–2407.
[41] S. Nakazono, Y. Imazaki, H. Yoo, J. Yang, T. Sasamori, N. Tokitoh, T. Cédric, H. Kageyama, D. Kim, H. Shinokubo, A. Osuka, *Chem. Eur. J.* **2009**, *15*, 7530–7533.
[42] S. Nakazono, S. Easwaramoorthi, D. Kim, H. Shinokubo, A. Osuka, *Org. Lett.* **2009**, *11*, 5426–5429.
[43] B. Zhang, H. Soleimaninejad, D. J. Jones, J. M. White, K. P. Ghiggino, T. A. Smith, W. W. H. Wong, *Chem. Mater.* **2017**, *29*, 8395–8403.
[44] G. Echue, G. C. Lloyd-Jones, C. F. J. Faul, *Chem. Eur. J.* **2015**, *21*, 5118–5128.
[45] X. An, T. Simmons, R. Shah, C. Wolfe, K. M. Lewis, M. Washington, S. K. Nayak, S. Talapatra, S. Kar, *Nano Lett.* **2010**, *10*, 4295–4301.
[46] M. Marcia, C. Vinh, C. Dolle, G. Abellán, J. Schönamsgruber, T. Schunk, B. Butz, E. Spiecker, F. Hauke, A. Hirsch, *Adv. Mater. Interfaces* **2016**, *3*, 1600365.
[47] A. Ziletti, A. Carvalho, D. K. Campbell, D. F. Coker, A. H. Castro Neto, *Phys. Rev. Lett.* **2015**, *114*, 046801.
[48] J. O. Island, G. A. Steele, H. S. J. van der Zant, A. Castellanos-Gomez, *2D Mater.* **2015**, *2*, 011002.
[49] Y. Zhao, Q. Zhou, Q. Li, X. Yao, J. Wang, Y. Zhao, Q. Zhou, Q. Li, X. Yao, J. Wang, *Adv. Mater.* **2017**, *29*, 1603990.
[50] M. Zhang, G. Zhao, *ChemSusChem* **2012**, *5*, 879–887.
[51] E. Fron, G. Schweitzer, P. Osswald, F. Würthner, P. Marsal, D. Beljonne, K. Müllen, F. C. De Schryver, M. Van der Auweraer, *Photochem. Photobiol. Sci.* **2008**, *7*, 1509–1521.
[52] V. Sivamurugan, K. Kazlauskas, S. Jursenas, A. Gruodis, J. Simokaitiene, J. V. Grazulevicius, S. Valiyaveettil, *J. Phys. Chem. B* **2010**, *114*, 1782–1789.
[53] J. Li, P. Li, M. Fan, X. Zheng, J. Guan, M. Yin, *Angew. Chem. Int. Ed.* **2022**, *61*, e202202532.
[54] C. Kohl, T. Weil, J. Qu, K. Müllen, *Chem. Eur. J.* **2004**, *10*, 5297–5310.
[55] C. D. Schmidt, C. Böttcher, A. Hirsch, *Eur. J. Org. Chem.* **2007**, *2007*, 5497–5505.
[56] D. Görl, X. Zhang, F. Würthner, *Angew. Chem. Int. Ed.* **2012**, *51*, 6328–6348.
[57] T. Heek, F. Würthner, R. Haag, *Chem. Eur. J.* **2013**, *19*, 10911–10921.
[58] Y. Ma, X. Li, X. Wei, T. Jiang, J. Wu, H. Ren, *Korean J. Chem. Eng.* **2015**, *32*, 1427–1433.
[59] L. Q. Xu, L. Wang, B. Zhang, C. H. Lim, Y. Chen, K.-G. Neoh, E.-T. Kang, G. D. Fu, *Polymer* **2011**, *52*, 2376–2383.
[60] C. Backes, F. Hauke, A. Hirsch, *Adv. Mater.* **2011**, *23*, 2588–2601.
[61] A. Hirsch, J. M. Englert, F. Hauke, *Acc. Chem. Res.* **2012**, *46*, 87–96.
[62] J. Cui, S. Zhou, *J. Nanopart. Res.* **2017**, *19*, 357.
[63] S. Wild, V. Lloret, V. Vega-Mayoral, D. Vella, E. Nuin, M. Siebert, M. Koleśnik-Gray, M. Löffler, K. J. J. Mayrhofer, C. Gadermaier, V. Krstić, F. Hauke, G. Abellán, A. Hirsch, *RSC Adv.* **2019**, *9*, 3570–3576.
[64] D. Hanlon, C. Backes, E. Doherty, C. S. Cucinotta, N. C. Berner, C. Boland, K. Lee, A. Harvey, P. Lynch, Z. Gholamvand, S. Zhang, K. Wang, G. Moynihan, A. Pokle, Q. M. Ramasse, N. McEvoy, W. J. Blau, J. Wang, G. Abellan, F. Hauke, A. Hirsch, S. Sanvito, D. D. O'Regan, G. S. Duesberg, V. Nicolosi, J. N. Coleman, *Nat. Commun.* **2015**, *6*, 8563.
[65] S. Walia, Y. Sabri, T. Ahmed, M. R. Field, R. Ramanathan, A. Arash, S. K. Bhargava, S. Sriram, M. Bhaskaran, V. Bansal, S. Balendhran, *2D Mater.* **2016**, *4*, 015025.
[66] T. Zhang, Y. Wan, H. Xie, Y. Mu, P. Du, D. Wang, X. Wu, H. Ji, L. Wan, *J. Am. Chem. Soc.* **2018**, *140*, 7561–7567.
[67] A. Castellanos-Gomez, L. Vicarelli, E. Prada, J. O. Island, K. L. Narasimha-Acharya, S. I. Blanter, D. J. Groenendijk, M. Buscema, G. A. Steele, J. V. Alvarez, H. W. Zandbergen, J. J. Palacios, H. S. J. Van Der Zant, *2D Mater.* **2014**, *1*, 025001.
[68] S. Demmig, H. Langhals, *Chem. Ber.* **1988**, *121*, 225–230.
[69] M. E. Pérez-Ojeda, N. Zink-Lorre, S. Pla, A. Zink, Á. Sastre-Santos, F. Fernández-Lázaro, A. Hirsch, *Dyes Pigm.* **2022**, *199*, 110044.
[70] K. Mahata, P. D. Frischmann, F. Würthner, *J. Am. Chem. Soc.* **2013**, *135*, 15656–15661.
[71] Z.-G. Zhang, B. Qi, Z. Jin, D. Chi, Z. Qi, Y. Li, J. Wang, *Energy Environ. Sci.* **2014**, *7*, 1699–1973.
[72] T. Deligeorgiev, D. Zaneva, I. Petkov, I. Timcheva, R. Sabnis, *Dyes Pigm.* **1994**, *24*, 75–81.
[73] M. Marcia, *PhD Thesis*, Friedrich-Alexander-University Erlangen-Nürnberg (Germany), **2017**■■Dear author, please check if you can mention a page number■■.

Manuscript received: June 4, 2024
Version of record online: ■■, ■■

RESEARCH ARTICLE

Perylene diimides have been used for passivating black phosphorus, however, a concrete set of tools for fine-tuning such an interaction remains elusive. Therefore, ten different PDIs were investigated. It could be shown, that especially water–soluble PDIs provide reliable functionalization and stabilizing capabilities as they passivate BP up to 35 days.

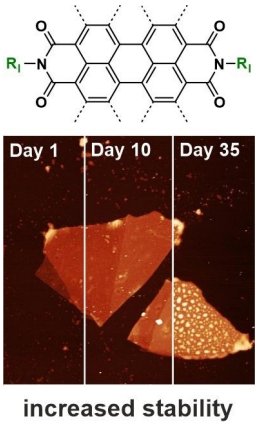

J. Eisenkolb, Dr. V. Lloret, N. Zink-Lorre, Dr. S. Pla, G. Abellán, Prof. Á. Sastre-Santos, Dr. F. Hauke, Prof. F. Fernández-Lázaro, Prof. A. Hirsch**

1 – 9

Investigations of Crucial Factors for the Non-Covalent Functionalization of Black Phosphorus (BP) using Perylene Diimide Derivatives for the Passivation of BP Nanosheets

SPACE RESERVED FOR IMAGE AND LINK

Share your work on X! Chemistry – A European Journal promotes selected articles on X (formerly known as Twitter). Each article post contains the title, name of the corresponding author, a link to the article, selected handles and hashtags, and the ToC picture. If you, your team, or your institution have an X account, please include its handle @username below. We recommend sharing and interacting with these posts through your personal and/or institutional accounts to help increase awareness of your work! Please follow us @ChemEurJ.

ORCID (Open Researcher and Contributor ID)

Please check that the ORCID identifiers listed below are correct. We encourage all authors to provide an ORCID identifier for each coauthor. ORCID is a registry that provides researchers with a unique digital identifier. Some funding agencies recommend or even require the inclusion of ORCID IDs in all published articles, and authors should consult their funding agency guidelines for details. Registration is easy and free; for further information, see http://orcid.org/.

Prof. Andreas Hirsch http://orcid.org/0000-0003-1458-8872
Prof. Ángela Sastre-Santos
Dr. Sara Pla
Dr. Frank Hauke http://orcid.org/0000-0001-9637-7299
Prof. Fernando Fernández-Lázaro
Gonzalo Abellán
Jasmin Eisenkolb
Dr. Vicent Lloret
Nathalie Zink-Lorre